Fermilab FERMILAB-Conf-01/072-T May 2001

W/Z + B$\overline{\text{B}}$/JETS AT NLO USING THE MONTE CARLO MCFM

J.M. CAMPBELL
Theory Department, Fermilab, PO Box 500,
Batavia, IL 60510, USA

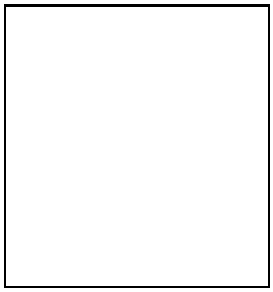

We summarize recent progress in next-to-leading QCD calculations made using the Monte Carlo MCFM. In particular, we focus on the calculations of $p\bar{p} \to Wb\bar{b}$, $Zb\bar{b}$ and highlight the significant corrections to background estimates for Higgs searches in the channels WH and ZH at the Tevatron. We also report on the current progress of, and strategies for, the calculation of the process $p\bar{p} \to W/Z + 2$ jets.

1 MCFM Background

With the advent of Run II at the Tevatron we will be able to perform detailed studies of femtobarn-level processes for the first time. The production of final states involving heavy quarks, leptons and missing energy is particularly interesting since these are common signatures for new physics beyond the Standard Model. For example, a light Higgs in the mass range 110 GeV$< m_H <$ 140 GeV predominantly decays into a $b\bar{b}$ pair. In order to assess search strategies and perform meaningful comparisons with the data, a solid knowledge of the Standard Model backgrounds is necessary. In an attempt to fill this need, the Monte Carlo program MCFM aims to provide a unified description of many of these femtobarn-level processes at next-to-leading order (in the strong coupling, α_S) accuracy. In many cases, the extension to NLO is made feasible by the recent calculations of virtual matrix elements involving a vector boson and four partons. [1]

The philosophy behind MCFM is somewhat similar to that of a general-purpose showering Monte Carlo such as Pythia [2] (although here we are of course working at a fixed order in α_S). One specifies a set of basic parameters and cuts, selects a process number from a table of included processes and then the Monte Carlo MCFM produces a set of relevant distributions. The main processes currently implemented at next-to-leading order are shown in Table 1, with various leptonic

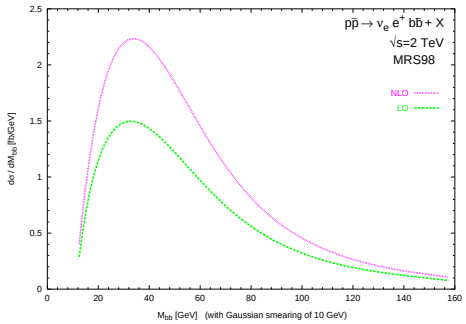

Figure 1: The $m_{b\bar{b}}$ distribution of the $W^+(\to \nu_e e^+)\, b\bar{b}$ background to the Higgs signal, at LO and NLO.

and hadronic decays of the bosons included as further sub-processes. Version 1.0 of the program is available for download at `http://www-theory.fnal.gov/people/campbell/mcfm.html`.

Table 1: The main processes included in `MCFM` at next-to-leading order.

$p\bar{p} \to W^{\pm}/Z$	$p\bar{p} \to W^+ + W^-$
$p\bar{p} \to W^{\pm} + Z$	$p\bar{p} \to Z + Z$
$p\bar{p} \to W^{\pm}/Z + H$	$p\bar{p} \to W^{\pm}/Z + 1$ jet
$p\bar{p} \to W^{\pm} + g^{\star}\ (\to b\bar{b})$	$p\bar{p} \to Zb\bar{b}$

2 Higgs Search Using `MCFM`

Studies using lowest-order Monte Carlos and other event generators show that for a Higgs in the mass range of 100-130 GeV, the most promising channels for discovery at Run II are associated Higgs production, [3]

$$p\bar{p} \longrightarrow W(\to e\nu)H(\to b\bar{b}),$$
$$p\bar{p} \longrightarrow Z(\to \nu\bar{\nu}, \ell\bar{\ell})H(\to b\bar{b}).$$

This mass region is particularly interesting in the light of recent hints from LEP2 suggesting a Higgs mass $m_H = 115$ GeV.

Considering first the WH signal, the main backgrounds are,

$$\begin{aligned} p\bar{p} &\longrightarrow W\, g^{\star}(\to b\bar{b}) \\ p\bar{p} &\longrightarrow W\, Z/\gamma^{\star}(\to b\bar{b}) \end{aligned} \qquad \begin{aligned} p\bar{p} &\longrightarrow t(\to bW^+)\bar{t}(\to \bar{b}W^-) \\ p\bar{p} &\longrightarrow W^{\pm *}(t(\to bW^+)\bar{b}) \\ qg &\longrightarrow q't(\to bW^+)\bar{b}. \end{aligned}$$

The signal, $Wg^{\star}$ and WZ backgrounds are calculable at the one-loop level in `MCFM` and the remainder at lowest order. In order to study the largest background - the continuum $Wg^{\star}$ - we introduce a set of standard cuts from the literature, [4] use a double b-tagging efficiency of $\epsilon_{b\bar{b}} = 0.45$ and employ the MRS98 set of parton distribution functions. [5] When searching for the Higgs signal, we are interested in the cross-section as a function of the $b\bar{b}$ pair mass, $m_{b\bar{b}}$. This distribution is compared at lowest order and next-to-leading order in Figure 1, with a renormalization and factorization scale $\mu = 100$ GeV. From examining this figure, one can see that the effect of the next-to-leading corrections is to increase the distribution by a factor of approximately 1.5 throughout, thus changing the shape very little.

The results of a parton-level study for $m_H = 110$ GeV, with all but the small $t\bar{t}$ and single-top backgrounds calculated at next-to-leading order, are summarized in Figure 2. It is clear from the

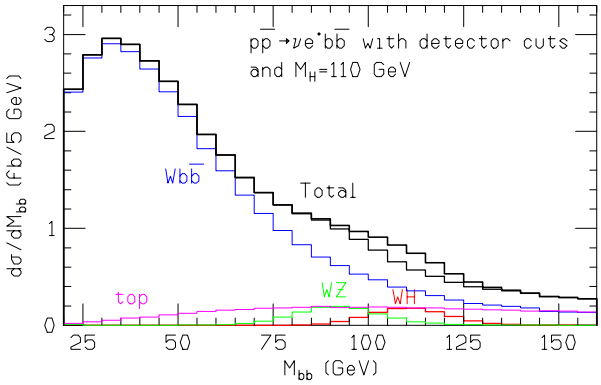

Figure 2: Parton-level signal and backgrounds assuming $m_H = 110$ GeV. The uppermost curve represents the signal+backgrounds, with the (almost identical) lower curve representing just the sum of all the backgrounds.

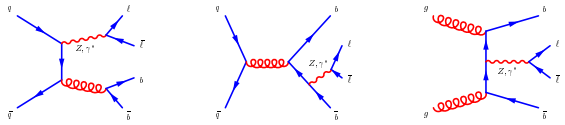

Figure 3: Sample diagrams contributing to the process $p\bar{p} \to Zb\bar{b}$. Diagram (c) represents a gauge-invariant set that does not appear at all in the $Wb\bar{b}$ calculation.

figure that the extraction of the Higgs signal requires detailed knowledge of the normalization and the kinematics of the backgrounds.

It is straightforward to perform a similar search in the ZH channel.[6] Here we shall concentrate on the $Z(\to \nu\bar{\nu})b\bar{b}$ background, calculated at next-to-leading order with `MCFM`, and compare with the $Wb\bar{b}$ calculation above. The Feynman diagrams required for this calculation - shown in Figure 3 - are very similar to the previous case, with additional contributions from gg initial states. These gg initial states are important for the Higgs search since they can readily produce a $b\bar{b}$ pair with a large invariant mass. For a conventional scale of 100 GeV, the $m_{b\bar{b}}$ distribution is shown in Figure 4. The effect of the radiative corrections is to produce a large K-factor ≈ 1.8 in the region of interest, $m_{b\bar{b}}$ from 100-130 GeV.

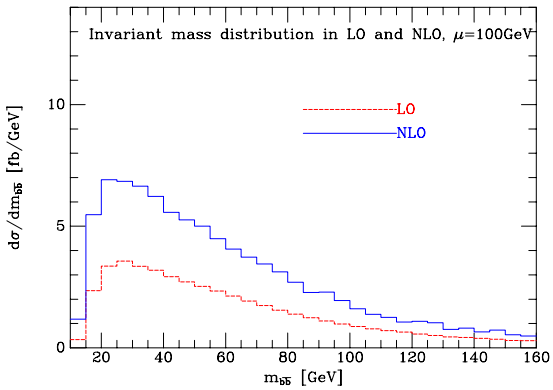

Figure 4: The $m_{b\bar{b}}$ distribution for the final state $Z(\to 3 \times \nu\bar{\nu})\, b\bar{b}$ at leading and next-to-leading order.

3 $W + 2$ jets: Work in Progress

The $p\bar{p} \to W + 2$ jets process can be viewed as an extension of the $Wb\bar{b}$ and $Zb\bar{b}$ calculations that have already been discussed in the previous sections. There are of course extra parton configurations that we must count, but the basic matrix elements (modulo couplings) are the same. Specifically, the $Wb\bar{b}$ calculation contains all the diagrams relevant for $q\bar{q} \to W + q'\bar{q}'$; the $Zb\bar{b}$ process, together with crossings, provides the $gg \to W + q\bar{q}$, $q\bar{q} \to W + gg$, $gq \to W + gq'$ and similar sub-processes. A further complication is that the contribution from the diagrams that include real radiation must incorporate the extra singularities due to more instances of soft or collinear gluons and collinear quark pairs. In order to simplify the calculation - and to reduce the required computation time - we have decided to employ a colour-decomposition of the matrix elements. In this procedure the matrix elements are expressed as an expansion in $1/N$ (where N is the number of colours, 3), with the hope that the sub-leading terms are small compared to the leading term. Performing the colour expansion we obtain ($V = W^{\pm}$, Z),

$$\begin{aligned} |\mathcal{M}_{NLO}(Vq\bar{q}gg)|^2 &\sim 1 \times \mathcal{G}_0 + \frac{1}{N^2} \times \mathcal{G}_2 + \frac{1}{N^4} \times \mathcal{G}_4 \\ |\mathcal{M}_{NLO}(Vq\bar{q}Q\bar{Q})|^2 &\sim \frac{1}{N} \times \mathcal{Q}_1 + \frac{1}{N^3} \times \mathcal{Q}_3 + \delta_{qQ} \left(1 \times \mathcal{Q}_0 + \frac{1}{N^2} \times \mathcal{Q}_2 \right) \end{aligned}$$

where the $\mathcal{G}_i$ and $\mathcal{Q}_i$ represent squared sub-amplitudes for the 2-quark and 4-quark processes respectively. Preliminary investigations suggest that the leading piece, $\mathcal{G}_0$ is both a good approximation to the full matrix element (including both processes) and considerably faster to run. For this reason, the inclusion of the term $\mathcal{G}_0$ has been the primary focus of the $W + 2$ jet calculation so far.

4 Conclusions

We have found large radiative corrections to the $Wb\bar{b}$ and $Zb\bar{b}$ processes. These results can significantly change estimates of the backgrounds to the processes $p\bar{p} \to WH$ and $p\bar{p} \to ZH$, which will be important search channels at the Tevatron. For the more general calculation of $W/Z + 2$ jet production, work is still ongoing but first results should be available soon.

Acknowledgements

I would like to thank my collaborator Keith Ellis. An EU grant to attend the Moriond conference is gratefully acknowledged.

References

1. Z. Bern, L. Dixon, D. Kosower and S. Weinzierl, *Nucl. Phys.* B **489**, 3 (1997);
   E. W. N. Glover and D. J. Miller, *Phys. Lett.* B **396**, 257 (1997);
   J. M. Campbell, E. W. N. Glover and D. J. Miller, *Phys. Lett.* B **409**, 503 (1997).
2. H.-U. Bengtsson and T. Sjöstrand, *Comp. Phys. Comm.* **46**, 43 (1987);
   T. Sjöstrand, *Comp. Phys. Comm.* **82**, 74 (1994).
3. A. Stange, W. Marciano, S. Willenbrock, *Phys. Rev.* D **49**, 1354 (1994); *Phys. Rev.* D **50**, 4491 (1994).
4. M. Carena *et al.*, Report of the Tevatron Higgs working group, hep-ph/0010338.
5. A. D. Martin, R. G. Roberts, W. J. Stirling and R. S. Thorne, *Euro. Phys. J.* C **4**, 463 (1998).
6. J. M. Campbell and R. K. Ellis, *Phys. Rev.* D **62**, 114012 (2000).